Shrinkage studies and optimization of multiplexed holographic lenses with high diffractive efficiency and wide angular response

Tomás Lloret, Marta Morales-Vidal, Belén Nieto-Rodríguez, José Carlos García-Vázquez, Manuel G. Ramírez, et al.

Tomás Lloret, Marta Morales-Vidal, Belén Nieto-Rodríguez, José Carlos García-Vázquez, Manuel G. Ramírez, Augusto Beléndez, Inmaculada Pascual, "Shrinkage studies and optimization of multiplexed holographic lenses with high diffractive efficiency and wide angular response," Proc. SPIE 12673, Optics and Photonics for Information Processing XVII, 126730E (4 October 2023); doi: 10.1117/12.2676470

SPIE.

Event: SPIE Optical Engineering + Applications, 2023, San Diego, California, United States

Shrinkage studies and optimization of multiplexed holographic lenses with high diffractive efficiency and wide angular response

Tomás Lloret[a], Marta Morales-Vidal[a,b], Belén Nieto-Rodríguez[a], José Carlos García-Vázquez[b], Manuel G. Ramírez[b,c], Augusto Beléndez[b,c], and Inmaculada Pascual[a,b]

[a]Departamento de Óptica, Farmacología y Anatomía, Universidad de Alicante, Carretera San Vicente del Raspeig s/n, 03690 San Vicente del Raspeig, Spain
[b]Instituto Universitario de Física Aplicada a las Ciencias y las Tecnologías, Universidad de Alicante, Carretera San Vicente del Raspeig s/n, 03690 San Vicente del Raspeig, Spain
[c]Departamento de Física, Ingeniería de Sistemas y Teoría de la Señal, Universidad de Alicante, Carretera San Vicente del Raspeig s/n, 03690 San Vicente del Raspeig, Spain

ABSTRACT

Today, the advancement of optical systems that can harness clean and renewable energy sources is a major focus for researchers and innovators worldwide. As we strive to create a sustainable future, this challenge has become increasingly critical to our success. Fresnel lenses are widely used as traditional concentrators, but they have a small acceptance angle, and the reflective elements need continuous maintenance of the surface reflectivity. Transmitting Holographic Optical Elements (HOEs) are an alternative to conventional lenses because they are more economical and versatile. Their material is usually a flexible photopolymer so that the optical element can be attached to different types of support, depending on whether one type of handling is required or another, and they tend to have low weight and volume, as well as a simple way of manufacturing. In addition, also provide an extended focusing area which helps to protect solar cells from heating damage. A theoretical and experimental study on the shrinkage of multiplexed holographic lenses (MHL) that were stored in a low-toxicity photopolymer was carried out. To accomplish the study, a K-space tool was used. Furthermore, an optimization analysis of the angular distance between peaks was performed. To determine efficiency, an evaluation of the short-circuit current under solar illumination with varying incident reconstruction angles was done.

Keywords: Holography, multiplexed holographic lenses, green photonics, high diffraction efficiency, wide acceptance angle

1. INTRODUCTION

Nowadays, concentrating photovoltaic (PV) technology is increasingly recognized as the most promising technology to meet the world's energy challenges. In order to obtain competitive photovoltaic energy, free-tracking, lightweight and low-cost systems must be achieved, and wavelengths that can damage the cell must be eliminated. Holographic optical elements (HOEs) are obtained using the holographic technique and can be an alternative to conventional lenses, as they are cheaper, lighter and more versatile than traditional Fresnel refractive lenses or parabolic mirrors. Different research groups have developed high-efficiency HSCs on photopolymers based on acrylamide, Bayfol, dichromated gelatin, silver halide, or photopolymers doped with nickel ions. This involves working with materials that present some toxicity. A.B. Sreebha et. al.[1] proposed in 2015 holographic lenses fabricated in silver halide using off-axis geometry to be employed in windows. With this material they achieved a diffraction efficiency of 33 % at 632.8 nm. Lee et al.[2] designed in 2016 a HSC based on the multiplexing of three holographic lenses (MHL3) on BayfolHX200, a low-thickness film (about 17 μm). The diffraction efficiency of 27%, 35%, and 23% at 532 nm was measured, and the acceptance angle achieved was 35°. S. Vorndran et al.[3] in

Further author information: (Send correspondence to T.L.)
T.L.: E-mail: tomas.lloret@ua.es

Optics and Photonics for Information Processing XVII, edited by Khan M. Iftekharuddin, Abdul A. S. Awwal, Victor Hugo Diaz-Ramirez, Proc. of SPIE Vol. 12673, 126730E · © 2023 SPIE · 0277-786X · doi: 10.1117/12.2676470

2016 fabricated using a spectrum-splitter photovoltaic module composed of two gelatin-based dichromated holographic lenses obtaining an acceptance angle of 38° and an average diffraction efficiency over the entire aperture around 85.4%. H. Akbari et.al[4,5] proposed in 2017 a system based on two diffractive optical elements (DOEs) prepared on 50 μm thickness acrylamide-based photopolymer with a 95% efficiency at 633 nm, but an average acceptance angle (12°). G. Aswathy et.al.[6] obtained in 2018 holographic concentrators based on holographic lenses recorded in a photopolymer material doped with nickel ions with diffraction efficiencies of 85% and with a small acceptance angle. They also obtained three MHLs with diffraction efficiencies of 77%, 15% and 1% with an acceptance angle of 10°. Finally, M. Morales-Vidal et. al[7] designed in 2022 a HSC based on 7 multiplexed holographic lenses (MHL7) on Biophotopol, the same material used in this work, in 197 μm layers. The average diffraction efficiency at 633 nm was 46.5% and the acceptance angle was 60°.

In this work, we demonstrate the valuable role of a low-toxicity photopolymer in advancing sustainable energy systems. Five MHLs have been recorded in a Biophotopol material with different angular separation between peaks ($\Delta\theta = 7.25°$, $\Delta\theta = 5.00°$, $\Delta\theta = 3.00°$) . A high-efficiency holographic solar concentrator, with an average diffraction efficiency of 85% and a good acceptance angle has been obtained from five peristrophic MHLs.

2. METHODS

2.1 Recording material

A low-toxicity hydrophilic material (Biophotopol photopolymer[8]) made-up of one monomer in a binder, an electron donor, and a dye sensitizer was used to record volume phase transmission MHLs. Biophotopol composition was developed using sodium acrylate (NaAO) as the monomer (NaAO was generated in situ through a reaction of acrylic acid (HAO) with sodium hydroxide (NaOH) in a 1:1 proportion), water as a unique solvent, triethanolamine (TEA) serving as the initiator and plasticizer, riboflavin 5'-monophosphate sodium salt (RF) serves as a dye, and polyvinyl alcohol (PVA) as a binder (Mw = 130,000 g/mol, hydrolysis grade = 87.7%). All compounds were purchased from Sigma-Aldrich Quimica SL (Madrid, Spain).

Table 1. Recording material composition quantities.

PVA (w/w %)	**NaAO (M)**	**TEA (M)**	**RF (M)**
11.3	0.49	$11.1{\cdot}10^{-3}$	$1.7{\cdot}10^{-3}$

The prepolymer solution was deposited in square glass molds 6.5 × 6.5 cm^2 (which have been previously washed and dried) by the force of gravity and left in dark inside an incubator (Climacell 111, Labexchange, Burladingen, Germany) overnight at a controlled relative humidity of 60 ± 5% and a temperature of 20 ± 1°C. The procedure was also carried out in a controlled light environment in which the photopolymer layer was not sensitive.

2.2 Holographic experimental setup and solar simulator

The experimental setup used in the holographic recording stage can be seen in Fig 1. A diode-pumped laser emitting at 473 nm was spatially filtered and then split into two secondary beams (object and reference) with an intensity ratio 1:1. The collimated reference beam impinge to the photopolymer, while the object beam passed through a refractive lens (RL) and the converging beam focalize at a distance $d_{\frac{RL-PL}{2}}$ reaching to the photopolymer surface with the same spot size as the reference beam (0.5 cm). The object and reference beams were recombined at the photopolymer with the same object and reference angle $\theta_o = \theta_r = 7.25°$ with respect to normal incidence. The sum of both intensities recording beam was 2.2 mW/cm^2, the exposure time was adjusted to obtain the maximum diffraction efficiency. The transmitted and diffracted intensity were mesured in real time while recording (with a He-Ne laser at with RF is not sensitive).

On the other hand, the experimental setup used to reconstruct the MHLs with the solar simulator can be seen in Fig 2. The MHLs were characterized with a broadband unpolarized source and a monocrystalline silicon photovoltaic cell (PHYWE 2,5x5 cm^2) by measuring the relative value of the short-circuit current under short-circuit conditions ($R = 0\ \Omega$). The solar simulator source emits a continuous AM1.5G solar spectrum (350-1800 nm). It was collimated to reconstruct the MHLs with the conjugated beam to obtain the real image (convergent

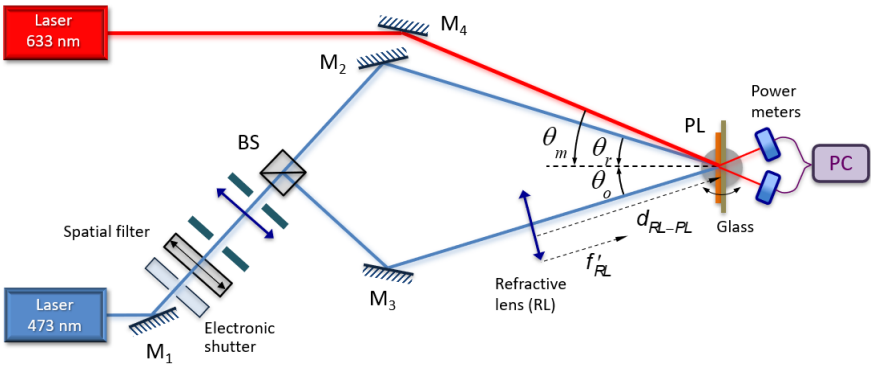

Figure 1. Experimental setup for recording multiplexed holographic lenses. BS: beam-splitter, M: mirrors, RL: refractive lens, PL: photopolymer layer.

beam). The diffracted beam of the HLs focuses the light on the photovoltaic cell as an extended focus (spectrum-splitting). The chromatic dispersion of this beam produces an aberrated image on the surface of the solar cell. This is due to the fact that each wavelength diffracts with a certain image angle and image focal length. The calculation of these parameters is given by equations (eq 1) and (eq 2), respectively.[9]

$$|\sin\theta_i| = |\sin\theta_c| + \mu\left(|\sin\theta_o| - |\sin\theta_r|\right) \tag{1}$$

$$\frac{1}{f'_{HL}} = \frac{1}{R_c} + \mu\left(\frac{1}{R_o} - \frac{1}{R_r}\right) \tag{2}$$

where i, c, o, r are the subscripts of the image, reconstruction, object and reference beams, respectively; and R is the distance from the source point to the hologram, respectively. Considering that the reference and reconstruction beams are plane waves, R_r and R tend to infinity, and R_o is the refraction focal length. Furthermore, f'_{HL} is the focal length of each lens, while μ is the ratio of the reconstruction wavelength to the recording wavelength $\mu = \lambda_c/\lambda_o$.

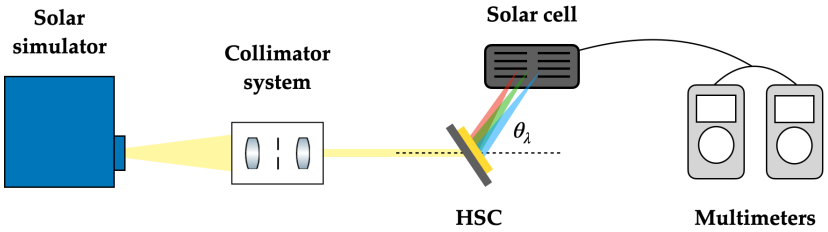

Figure 2. Solar-simulator reconstruction.

3. THEORETICAL BACKGROUND

3.1 Average diffraction efficiency

The parameter used par excellence to characterize diffraction holographic gratings and HLs is the diffraction efficiency. Diffraction efficiency (η) describes the amount of optical power diffracted by a hologram at a desired wavefront. Specifically, it is defined as the diffracted irradiance (E_d) in one or more diffraction orders relative to the incident irradiance (E_i) on the hologram. According to this definition:

$$\eta_i = \frac{E_d}{E_i} = \frac{P_d/A}{P_i/A} = \frac{P_d}{P_i} \tag{3}$$

where P_d is the diffracted optical power at the $i-th$ order, P_i is the incident power on the hologram, and A is the surface area of the photodetector. To avoid having to make corrections in the calculation of η (absorption losses, Fresnel reflections, etc), a good method is to consider the following definition:

$$\eta_i = \frac{P_d}{P_d + P_t} \tag{4}$$

where P_t is the transmitted power, so instead of considering the incident power, the sum of the diffracted and transmitted power is considered. In this work this definition was used to analyze the diffraction efficiency experimentally.

When multiplexing holograms, the average diffraction efficiency must be calculated. First, the dynamic range is defined as the number of holograms of diffraction efficiency $\eta = 1$ (100 %) that can be stored in a material with a given thickness.[10] The mathematical expression is as follows:

$$M\# = \sum_{i=1}^{N} \eta_i^{1/2} \tag{5}$$

where η_i is the diffraction efficiency of each hologram and N the number of holograms stored. Once the dynamic range has been calculated, it could be deduced how many holograms can be stored in that recording material with a given diffraction efficiency, or in other words, with what diffraction efficiency the holograms would be recorded if a certain number of them were stored. For this purpose, the average diffraction efficiency (η_{AVR}) is defined as follows:

$$\eta_{AVR} = \left(\frac{M\#}{N}\right)^2 \tag{6}$$

3.2 Shrinkage model

One of the most important aspects of volume holograms is that the recording material can change over time. Generally, there can be a shrinkage of the material and this causes a period variation. To study thickness variations, A. Beléndez, et.al[11] studied thickness variations by using a T_e/N parameter defined as:

$$\frac{T_e}{N} = \frac{\sin(\theta_r) + \sin(\theta_o)}{2\sin(\theta_c) + \mu\left[\sin(\theta_o) - \sin(\theta_r)\right]} \tag{7}$$

where T_e is the physical thickness of the photopolymer and $N = n_c/n_r$ represents the effective refractive index. Two cases can be deduced from the above expression.

In the case where the object and reference beams are symmetric with respect to the normal to the sample ($\theta_o = -\theta_r$), $T_e/N = 0$, and therefore as the fringes of the interferential pattern etched into the material are perpendicular to the plane in which it is located, any variation in thickness will be uniformly distributed without affecting the modification of the pattern.

However, in the case where the object and reference beams are asymmetric with respect to the normal to the sample ($\theta_o \neq -\theta_r$), the opposite is true. In this case, $T_e/N \neq 0$ and the interference pattern recorded during the recording stage forms a certain angle with the plane in which the material is located, and this means that the changes generated in the thickness of the material can cause a rotation of the fringes stored in the medium, as well as a change in their spacing, and the reconstruction geometry and/or wavelength must be modified so that the Bragg condition can be fulfilled during the hologram reconstruction.

To study this phenomenon, the geometrical approximation proposed by R. Fernández, et.al[12] has been used. The recorded fringes are represented by continuous lines and separated by a spatial period Λ. The fringes after shrinkage are represented by dashed lines and separated by a new period Λ'; d is the initial optical thickness and d' the thickness after shrinkage; Moreover, Λ_x and L_x are considered two constants that are independent of

shrinkage and can be considered equal. Let us see how, starting from the geometry described by R. Fernández, et.al,[12] the expressions for the calculation of the new period ($\Lambda^{'}$) after shrinkage can be deduced.

The following relationships can be obtained:

$$\frac{\Lambda^{'}}{\Lambda_x} = \sin(\phi) \tag{8}$$

$$\frac{d}{L_x} = \tan(\phi) \tag{9}$$

The following expressions can be derived from the geometry:

$$\Lambda^{'} = \Lambda \frac{\sin(\phi^{'})}{\sin(\phi)} \qquad d^{'} = d\frac{\tan(\phi^{'})}{\tan(\phi)} \tag{10}$$

$$\Delta\Lambda = \Lambda - \Lambda^{'} \qquad \Delta d = d^{'} - d \tag{11}$$

Experimentally, the physical and optical thickness was measured before and after the curing process.[13]

4. RESULTS

First, average diffraction efficiencies and acceptance angles were analyzed for five MHLs under three different conditions (see Fig 3). Those conditions were with peak-to-peak separation angles around $\Delta\theta = 7.25^o$, $\Delta\theta = 5.00^o$ and $\Delta\theta = 3.00^o$, respectively. The average diffraction efficiency was obtained by reconstructing the MHLs with the He-Ne laser, while the acceptance angle was obtained by reconstructing with the solar simulator illumination. Three MHL5 were obtained with $\eta_{AVR} = 73\%$ (Fig 3a) and $\theta_{acc} = 50^o$ (Fig 3b), $\eta_{AVR} = 82\%$ (Fig 3c) and $\theta_{acc} = 38^o$ (Fig 3d), $\eta_{AVR} = 85\%$ (Fig 3e) and $\theta_{acc} = 26^o$ (Fig 3f), respectively. It can be seen how as the angular distance between peaks decreases when reconstructing with the solar simulator, the peaks merge until finally, for $\Delta\theta = 3.00^o$, all peaks merge into the same optimized envelope curve. It is also seen that the smaller the inter-peak angle, the higher the diffraction efficiency.

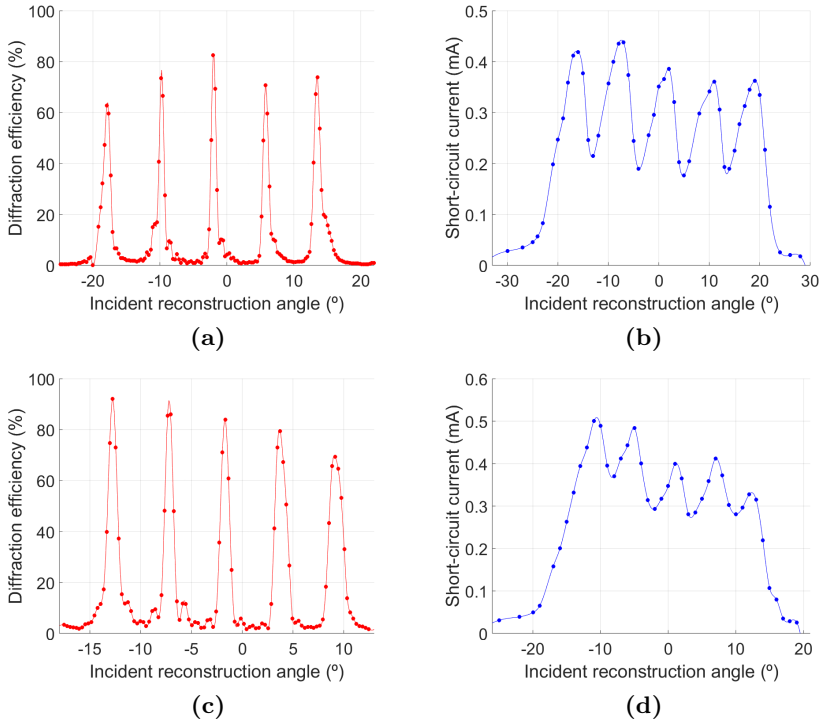

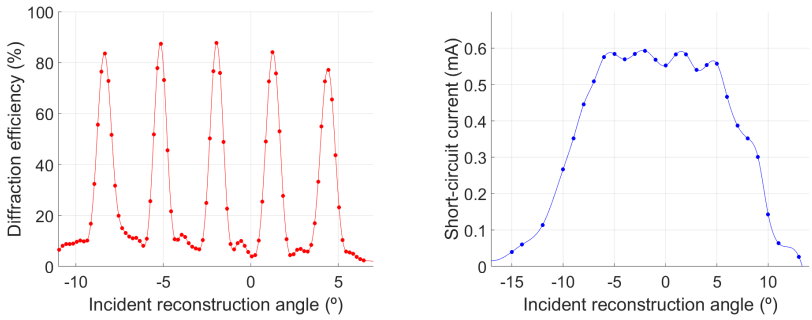

(e) **(f)**

Figure 3. Solar concentrator based on five MHLs. Reconstruction with 633 nm laser. **(a)** $\Delta\theta = 7.25^o$, **(c)** $\Delta\theta = 5.00^o$, **(e)** $\Delta\theta = 3.00^o$. Reconstruction with solar simulator illumination. **(b)** $\Delta\theta = 7.25^o$, **(d)** $\Delta\theta = 5.00^o$, **(f)** $\Delta\theta = 3.00^o$.

Table 2. Resumen de las variaciones de espesor óptico y periodo debidos al estudio del *shrinkage*.

$\boldsymbol{\Delta\theta = 7.25^o}$					
N LH	**1**	**2**	**3**	**4**	**5**
$\boldsymbol{\Delta d\ (\mu m)}$	7	3	9	10	8
$\boldsymbol{\Delta\Lambda\ (\mu m)}$	$9 \cdot 10^{-4}$	0	$8 \cdot 10^{-4}$	$3.5 \cdot 10^{-3}$	$6 \cdot 10^{-3}$
$\boldsymbol{\Delta\theta = 5.00^o}$					
N LH	**1**	**2**	**3**	**4**	**5**
$\boldsymbol{\Delta d\ (\mu m)}$	11	10	12	9	11
$\boldsymbol{\Delta\Lambda\ (\mu m)}$	$2 \cdot 10^{-4}$	$2 \cdot 10^{-4}$	$1.1 \cdot 10^{-3}$	$2.2 \cdot 10^{-3}$	$5.3 \cdot 10^{-3}$
$\boldsymbol{\Delta\theta = 3.00^o}$					
N LH	**1**	**2**	**3**	**4**	**5**
$\boldsymbol{\Delta d\ (\mu m)}$	5	7	9	7	8
$\boldsymbol{\Delta\Lambda\ (\mu m)}$	0	0	$7 \cdot 10^{-4}$	$1.1 \cdot 10^{-3}$	$2 \cdot 10^{-3}$

Finally, to study the stability of the holographic concentrators, the shrinkage phenomenon was studied. For this purpose, the physical thickness was measured before and after the curing process, and the optical thickness of each MHL was adjusted using the Kogelnik Coupled Wave Analysis. With these thicknesses, equations (10 and 11) were used to obtain the new period Λ'. Table 2 represents the data for the MHL5 cases with $\Delta\theta = 7.25^o$, $\Delta\theta = 5.00^o$ and $\Delta\theta = 3.00^o$, respectively. It can be observed that in the steeper strips, there are higher period variations. In Table 2, making to the case $\Delta\theta = 7.25^o$, it can be observed that the lowest variation of thickness and period occurs for the symmetric HLs, while these variations increase in the more asymmetrical HLs. With respect to the two cases ($\Delta\theta = 5.00^o$, $\Delta\theta = 3.00^o$), the more asymmetric the stored HLs are, the higher the variation of thickness and period, being lower in the cases closer to the symmetric configuration. This is important to take into account when large acceptance angles are required, since then the last stored HLs would present high asymmetries and therefore significant variations in thickness and period.

5. CONCLUSIONS

As a conclusion of this work, we can remark that three holographic solar concentrators based on five MHLs in a low toxicity photopolymer have been obtained. In order to increase the acceptance angle and diffraction efficiency of the current holographic concentrators, five MHLs were recorded with an angular separation between peaks of $\Delta\theta = 7.25^o$, $\Delta\theta = 5.00^o$ and $\Delta\theta = 3.00^o$. The average diffraction efficiencies achieved were 73%, 82% and 85% at a reconstruction wavelength of 633 nm. In addition, the angular widths obtained by white light from a solar simulator were 26°, 38° and 50°. Furthermore, considering the importance of the shrinkage with asymmetric recording stages, it was observed that when the recordings are more asymmetrics, the shrinkage was greater. However, it was seen that this phenomenon was not significant in the cases studied.

ACKNOWLEDGMENTS

This research was funded by Universidad de Alicante (UAFPU20-23); Generalitat Valenciana (CIDEXG/2022/60, IDIFEDER/2021/014, PROMETEO/2021/006); Ministerio de Ciencia e Innovación (PID2019-106601RB-I00, PID2021-123124OB-I00).

REFERENCES

[1] Sreebha, A. B., Mahadevan Pillai, V. P., and Ajith Kumar, P. T., "Development of a window holographic lens to utilize solar energy," in [*Advances in Optical Science and Engineering*], Lakshminarayanan, V. and Bhattacharya, I., eds., 141–145, Springer India, New Delhi (2015).

[2] Lee, J. H., Wu, Y., Piao, M., and Kim, N., "Holographic solar energy concentrator using angular multiplexed and iterative recording method," *IEEE Photonics J.* **8**, 1–11 (2016).

[3] Vorndran, S. H., Chrysler, B., Wheelwright, B., Angel, R., Holman, Z., and Kostuk, R., "Off-axis holographic lens spectrum-splitting photovoltaic system for direct and diffuse solar energy conversion," *Applied Optics* **55**, 7522–7529 (2016).

[4] Akbari, H., Naydenova, I., and Martin, S., "Using acrylamide-based photopolymers for fabrication of holographic optical elements in solar energy applications," *Appl. Opt.* **53**, 1343–1353 (Mar 2014).

[5] Akbari, H., Naydenova, I., Ahmed, H., McCormack, S., and Martin, S., "Development and testing of low spatial frequency holographic concentrator elements for collection of solar energy," *Sol. Energy* **155**, 103–109 (2017).

[6] Aswathy, G., Rajesh, C. S., Sreejith, M. S., Vijayakumar, K. P., and Kartha, C. S., "Designing photovoltaic concentrators using holographic lens recorded in nickel ion doped photopolymer material," *Sol. Energy* **163**, 70–77 (2018).

[7] Morales-Vidal, M., Lloret, T., Ramírez, M. G., Beléndez, A., and Pascual, I., "Green and wide acceptance angle solar concentrators," *Optics Express* **30**, 25366–25378 (2022).

[8] Ortuño, M., Fernández, E., Gallego, S., Beléndez, A., and Pascual, I., "New photopolymer holographic recording material with sustainable design," *Opt. Express* **15**, 12425–12435 (Sep 2007).

[9] Latta, J. N., "Computer-based analysis of hologram imagery and aberrations. i. hologram types and their nonchromatic aberrations," *Appl. Opt.* **10**(3), 599–608.

[10] Fernández, E., Ortuño, M., Gallego, S., García, C., Beléndez, A., and Pascual, I., "Comparison of peristrophic multiplexing and a combination of angular and peristrophic holographic multiplexing in a thick pva/acrylamide photopolymer for data storage," *Appl. Opt.* **46**, 5368–5373 (Aug 2007).

[11] Beléndez, A., Pascual, I., and Fimia, A., "Model for analyzing the effects of processing on recording material in thick holograms," *J. Opt. Soc. Am. A* **9**, 1214–1223 (Jul 1992).

[12] Fernández, R., Gallego, S., Navarro-Fuster, V., Neipp, C., Francés, J., Fenoll, S., Pascual, I., and Beléndez, A., "Dimensional changes in slanted diffraction gratings recorded in photopolymers," *Opt. Mater. Express* **6**, 3455–3468 (Nov 2016).

[13] Ramírez, M. G., Sirvent, D., Morales-Vidal, M., Ortuño, M., Martínez-Guardiola, F. J., Francés, J., and Pascual, I., "Led-cured reflection gratings stored in an acrylate-based photopolymer," *Polymers* **11**(4) (2019).